Toward Ex Situ Phase-Encoded Spectroscopic Imaging

VASILIKI DEMAS,[1, 2] CARLOS MERILES,[3] DIMITRIS SAKELLARIOU,[4] SONG-I HAN,[5] JEFFREY REIMER,[2] ALEXANDER PINES[1]

[1] *Department of Chemistry, University of California, Materials Sciences Division, Ernest Orlando Lawrence Berkeley National Laboratory, D62 Hildebrand, Berkeley, California 94720*
[2] *Department of Chemical Engineering, University of California, Berkeley, California 94720*
[3] *Department of Physics, City College of New York (CUNY), New York, New York 10031*
[4] *Laboratoire Claude Fréjacques, CEA Saclay/DSM/DRECAM/SCM-CNRS URA 331, Gif-sur-Yvette 91191, France*
[5] *Chemistry and Biochemistry, University of California, Santa Barbara, California*

ABSTRACT: Spectroscopic imaging of a sample placed outside of both the radio frequency and the imaging gradient coils is presented. The sample is placed in a field with a permanent one-dimensional inhomogeneity. The imaging gradients used for phase encoding are designed to produce a static field that depends only on the transverse direction, uncoupling the effects associated with the single-sided nature of these coils. Two-dimensional imaging coupled with chemical shift information is obtained via the ex situ matching technique. Open-saddle geometry is used to match the static field profile for chemical shift information recovery. Concepts Magn Reson Part B (Magn Reson Engineering) 29B: 137–144, 2006

KEY WORDS: ex situ; single sided; low field; inhomogeneous fields; spectroscopic imaging; RF matching

INTRODUCTION

Nuclear magnetic resonance spectroscopy (NMR) can nondestructively sense molecular dynamics, chemical identity, transport phenomena, and mechanical properties. Magnetic resonance imaging (MRI) can penetrate deep within most nonmetallic objects to yield images and spatially targeted spectra. Despite its utility, the requirements for conventional NMR limit the type of systems that can be studied, demanding small samples, inserted inside massive superconducting magnets in the laboratory, to ensure a homogeneous static magnetic field in the case of spectroscopy and well-controlled gradients in the case of imaging. The development of outside-the-magnet or "ex situ" spectroscopy and imaging would empower field deployment of magnetic resonance. These same technologies would also ease present restrictions on sample size and enable remote scanning of objects, as well as reduce the cost of NMR/MRI systems for chemical analysis and online product quality control. The benefits of such technologies have long been recognized, and a continuous effort to improve both the devices and the methods are being made. Nonconventional NMR imaging and relaxation measurements are being done routinely with devices such as the NMR MOUSE and other unilateral sensors (*1–8*). Recently, spectroscopy and spectroscopic imaging in emulated ex-situ conditions have been conducted, and the first high-resolution spectrum in a one-sided low-field system was obtained using the ex-situ matching methodology (*9–12*).

Received 27 February 2006; revised 24 April 2006; accepted 27 April 2006

Correspondence to: Vasiliki Demas; E-mail: vdemas@berkeley.edu

Concepts in Magnetic Resonance Part B (Magnetic Resonance Engineering), Vol. 29B(3) 137–144 (2006)

Published online in Wiley InterScience (www.interscience.wiley.com). DOI 10.1002/cmr.b.20069

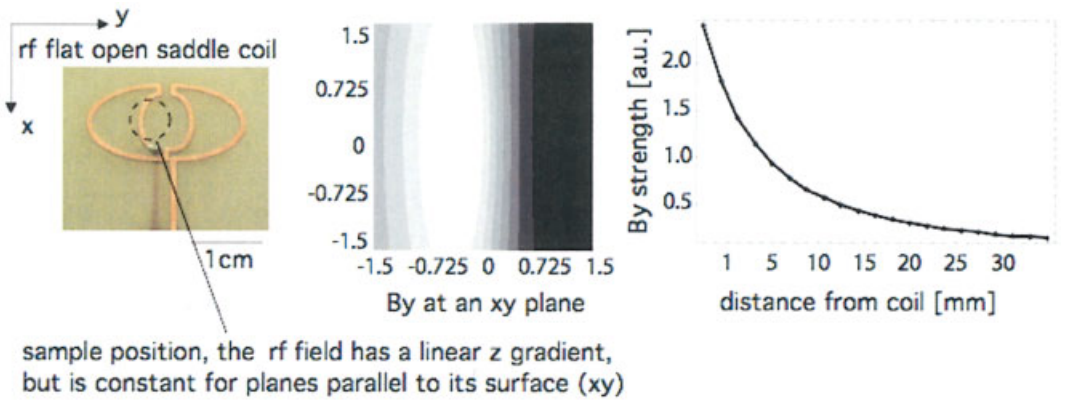

Figure 1 The layout of the RF coil (left). Simulation results for the y component of the magnetic field formed by the coil are shown on the right, in an xy plane 5 mm away from the coil (middle). These are contours half an inner radius away from the coil. Not shown, the x and z components are inhomogeneous in the area where the sample is placed, but they are three orders of magnitude smaller than the y component, which is homogeneous for that sample region. Also shown is the dependence of the y component along z (away from the coil). The units shown for the value are arbitrary, but the maximum field strength was measured to be 1 Gauss (for 100W of power). [Color figure can be viewed in the online issue, which is available at www.interscience.wiley.com.]

In this article we present high-resolution spectroscopy correlated with image information in a one-sided NMR probe, where the sample is placed outside both the RF and the imaging gradient coils, in the presence of a constant one-dimensional static field inhomogeneity. The imaging gradients used for phase encoding are designed to produce a static field that depends only on the transverse direction. This allows for volume imaging as opposed to slice selection imaging. It is a further step toward our final goal (i.e., phase-encoded portable spectroscopic imaging [PEPSI]) while still using an artificially inhomogeneous magnet. Existing "inside-out" and portable NMR systems possess large nonlinear gradients in more than one direction, which make the application of the ex-situ matching technique challenging (*9–11*). Considerable effort is expended toward designing hardware, such as developing dedicated RF-coil geometries suitable for one-sided magnets, custom-made electromagnets, permanent magnets, and one-sided superconducting magnets to allow the technique to be used in real ex-situ situations (*12–14*). Application of ex situ in a real one-sided system has yielded promising preliminary results (*12*). Efforts in methodology development are also underway (*15*). Our goal here is to describe the hardware design construction and results of a system with a flat saddle RF and ladder gradient coils to produce an RF gradient matched to the static field gradient in combination with well-controlled transverse gradients for imaging.

EQUIPMENT DESIGN

One of the requirements for the realization of an ex-situ matching experiment is to have the RF field matched with the static field, meaning that both fields should have a similar space dependence. For any given system, the coil-magnet design should be such that the correlation is linear, even if the individual field decays are nonlinear in space. Nonlinear correlations can also be accommodated by pulse sequence design (*15*).

In the work presented herein, we approach the scenario of a one-sided magnet with a gradient along the direction of the field (the field drops as we move away from the surface where the sample is placed). In a traditional high-field NMR instrument we created an inhomogeneity along the z direction to emulate the single-sided portable NMR system. The ex-situ methodology requires that the RF field be perpendicular to the static field and decay along the same direction. In the work presented here, the first experimental trial used a conical saddle coil to produce the required RF field, which has now evolved to the current open, truly single-sided saddle coil. This open-saddle geometry creates an intense RF field parallel to the plane of the coil, as shown in Fig. 1. This transverse field is constant in the x and y directions over the region where the sample is placed. There are some nonidealities in the design, as shown in the contour plot, but for a

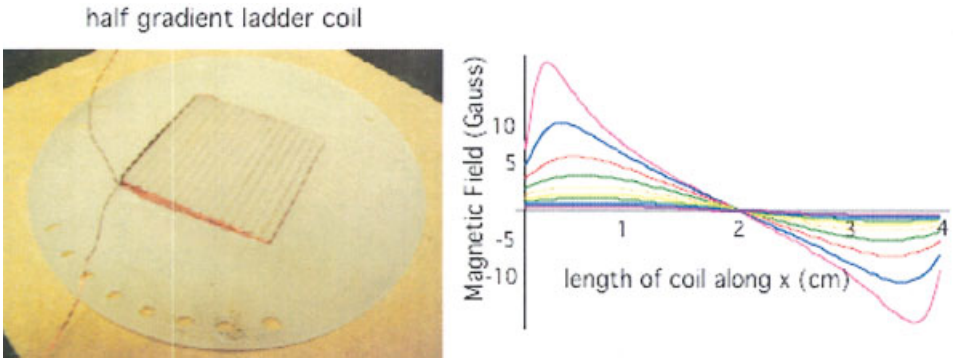

Figure 2 Left: photograph of a ladder gradient coil. The full ladder gradient set has two coils like the one shown here, positioned in the opposite direction (see diagram in Fig. 4), ensuring that the x gradient is centered in the middle of the overall setup. Right: the simulated z component of the magnetic field produced when a 1 Amp current flows through the coil. Gradients at various distances from the coil through the length of the coil are shown (the lines in the plot are from 0.6 cm from the surface of the coils, and 1 to 5 in increments of 0.5 cm). The stronger gradient (violet) is closest to the coils, and it decreases as we move away from them. The inductance of the each gradient coil set (two ladder pair) was about 4 μH. [Color figure can be viewed in the online issue, which is available at www.interscience.wiley.com.]

specified distance from the coil the y component of the magnetic field produced in the center of the coil is homogeneous. The x and y components are not homogeneous, but they are three orders of magnitude smaller than the x and z components. The B_1 field decays along the z axis in a linear fashion for that region containing the sample. Imaging with or without spectroscopic correlation requires gradient coils that yield linear gradients along a single dimension for all directions that need to be imaged. For example, a simple flat coil will produce field gradients in more than one spatial direction, a particularly vexing problem when one is considering single-sided magnet systems. This is not a problem when, due to large ex-situ gradients, only a small slice of the sample is excited, but becomes an issue if one corrects for the main static gradient (*13*, *16–18*). This will come into account for volume imaging in single-sided systems, and it is the main focus of the work presented here. Consider a simple double-ladder coil such as the one shown in Fig. 2 (*19*). This coil will produce a desirable gradient in the x direction, but the gradient will also depend on the z direction, thereby distorting the resulting image. As we move to slices of the sample away from the coil surface, the gradient is smaller, resulting in a narrower image. The phase gained by an element at position (x, z) by the first, ϕ_1, and second, ϕ_2, gradients separately is dependent on both the x and z position; however the total phase (subtracting the effect of the second gradient from the first), ϕ_{total}, is determined by only the x position (Eq. [1]). If, however, a second double-ladder coil at a distance Δz from the first ladder coil is arranged such that the current supplied is opposite to the first ladder coil, one can correct for the unwanted z gradient. This is shown in more detail in Fig. 3, where the results of a simple density matrix calculation show the distortions present for the case where a ladder coil produces x and z gradients. Figure 3(A) shows the image of a sphere when a standard gradient is present (the gradient depends on one coordinate). Figure 3(B) shows the case where the gradient has a dependence on more than one coordinate, as would be the case for single-sided gradient (one is the desired and the second is the one caused by the natural decay away from single-sided geometries), and Fig. 3(C) is the image by "double" single gradients (i.e., two identical sets of coils whose combined field is a pure one dimensional gradient). One can extrapolate this technique to other single-sided gradient coils:

$$\phi_1 = Gxzt \qquad [1.1]$$

$$\phi_2 = Gxz't, \text{ where } z' = z + \Delta z \text{ (coordinate transformation)} \qquad [1.2]$$

$$\phi_{total} = Gx\Delta zt \qquad [1.3]$$

With these geometries, the gradient and RF coils can be located underneath the sample (Fig. 4). The RF coil is shown to be positioned immediately underneath the

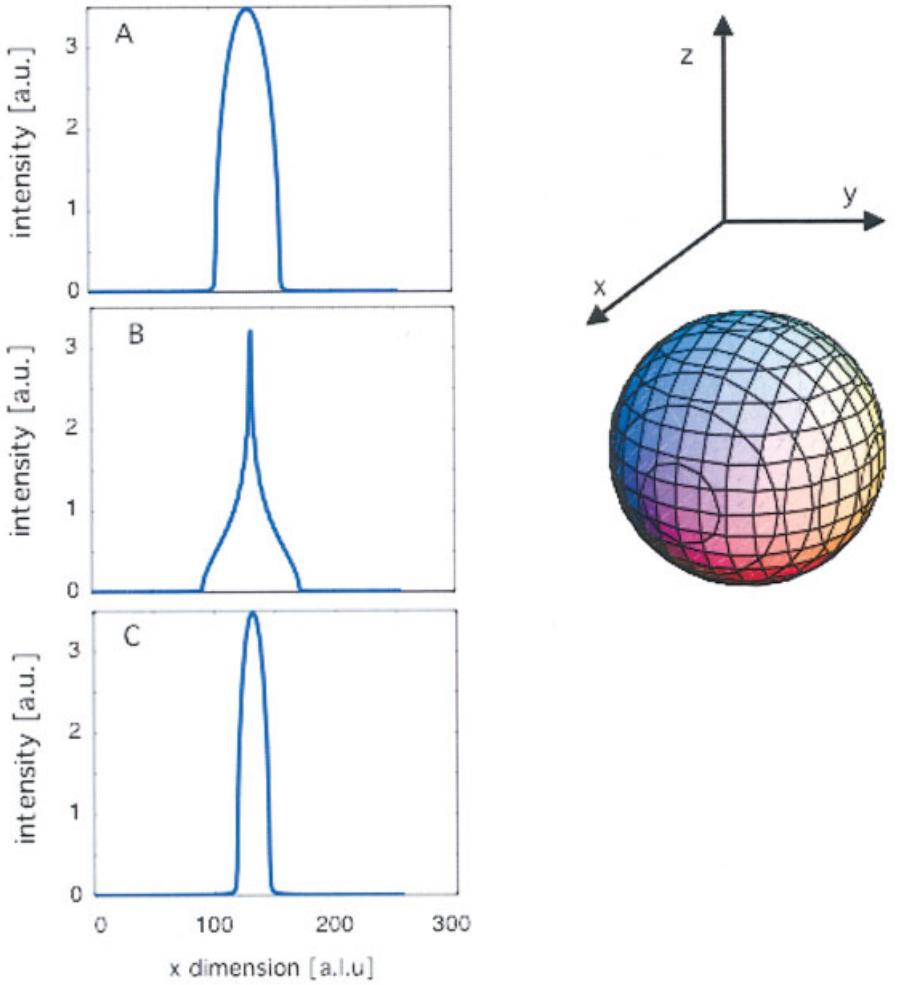

Figure 3 (A) Standard one-dimensional image of a sphere. Here we assume a "perfect" constant gradient. (B) One-dimensional image of the same sphere with a gradient along one side (here we assumed x) that has a coupled dependence on z (the dimension away from the gradient coils). (C) The corrected image. The field of view of the image is larger because the overall gradient has decreased for the same amount of current. [Color figure can be viewed in the online issue, which is available at www.interscience.wiley.com.]

sample. Two sets of gradients are placed under the RF coil (gradient set 1 and 2 as shown in Fig. 4). In Fig. 4, the reader can also see that each gradient set consisted of two ladders (named ladder and opposite coil). Each ladder was 4 × 4 cm and had 16 turns. Finally, a compressed solenoid coil of 5 cm diameter placed under the second x-gradient coil was used to induce a fixed gradient along the z axis emulating ex-situ conditions. A finite element calculation was used to determine the magnetic fields due to the ladder and saddle coils. The designs however, are intuitive, and a small number of parameters were varied for manual optimization of the final design (e.g., number of steps, width, and total length).

EXPERIMENTAL

The pulse sequence used for the experiments has been described previously and is shown in Fig. 5 (*11*). It consists of a conventional hard excitation pulse followed by a delay, $\tau = 8$ ms, and two adiabatic π pulses, each 4 ms long, separated by double the time interval, 2τ. The maximum amplitude of the first adiabatic pulse is scaled by a value λ relative to the maximum amplitude of the second adiabatic pulse. The overall phase given to the signal after the application of two adiabatic pulses with the same frequency sweep but different maximum amplitude is proportional to the RF field and a scaling factor λ but

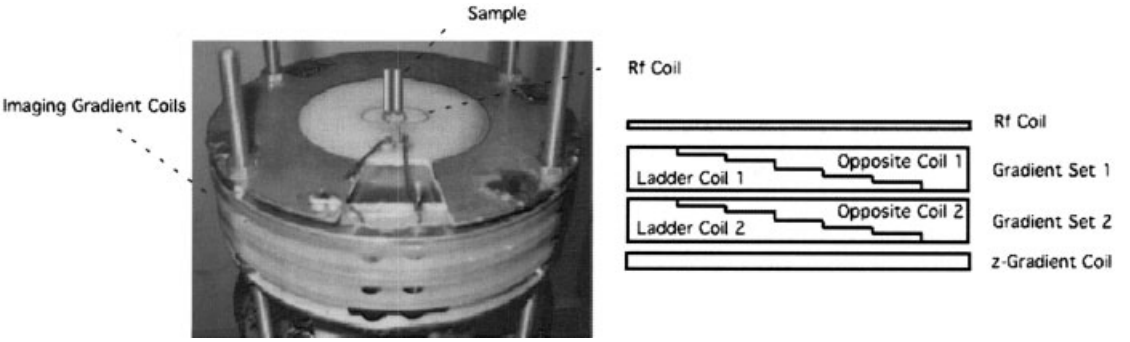

Figure 4 Experimental setup: the RF coil is an open saddle coil, producing a field parallel to its surface. The gradient coils placed underneath it are two sets of opposing ladder coils producing constant gradients along the x direction. (To simplify the drawing, the sketch on the right does not have the correct amount of steps.) There are 16 steps in each ladder coil in order to obtain the linear profile close to the coils and increase the gradient strength. An additional compressed solenoidal gradient coil is used to produce a static field inhomogeneity along the z direction. A cartoon of two tubes is added in the photograph to show where the samples were placed. The samples consisted of two capillary tubes, one filled with water and the other with oil, and they were placed over the region where the correlation holds.

is independent of the frequency offset $\Delta\omega = \omega_0 - \omega_1$ as long as it is within the range where the adiabatic condition holds (*8*, *10*, *12*, *13*).

Experiments were conducted in a superwide bore 180-MHz (4.2 T) magnet. A one-dimensional gradient along the z direction (G_z = 2 G/cm) is applied throughout the experiment to emulate the inherent inhomogeneity of a true ex-situ magnet. The gradient is produced by a compressed solenoid coil of 5 cm diameter placed 2 cm below the sample. The gradient, even though not linear overall (standard field decay), was assumed to be approximately linear over the region where the sample was placed. The amplitude of the gradient pulses along the x direction is varied to obtain image information along this dimension. Eighty phase encoding steps (the step gradient value was 0.025 G/cm) were performed, and a complete set of imaging experiments is repeated for 50 different values of λ (λ is incremented between 1 and 0.8). For each scaling value λ, B_1 inhomogeneities compensate for B_0 inhomogeneities, but the refocusing corresponds to a different evolution time for the chemical shift. Incrementing λ thus introduces a new time-domain dimension for chemical shift evolution, which, after Fourier transformation, yields the NMR spectral information (*10*).

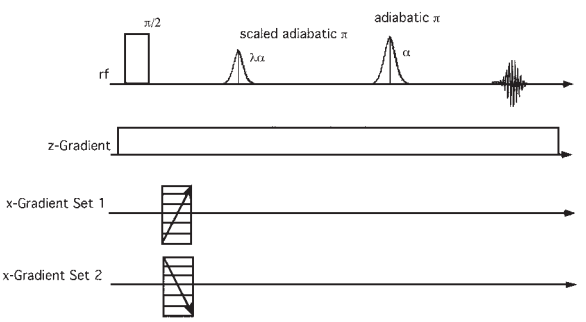

Figure 5 Pulse sequence: the RF instructions consist of a conventional hard excitation pulse, followed by a delay, τ = 8 ms, and two adiabatic π pulses, each 4 ms long, separated by double the time interval, 2τ. The maximum amplitude of the first adiabatic pulse is scaled by a value λ relative to the maximum amplitude of the second adiabatic pulse. The z-gradient coil is persistent during the sequence to emulate the inhomogeneity inherent in single-sided systems. Gradients along the x direction for phase encoding were implemented using the two-ladder gradient sets. The two sets are pulses at the same time, with reversed polarity.

SIMULATIONS

We have simulated the application of this pulse sequence to a virtual spherical sample containing two chemical species placed in the setup described above, with a constant one-dimensional linear gradient in both the static and the RF field (Fig. 6[A]). Figure 6(B) shows the correlation data. The correlation for the matched B_1 and B_0 field gradients displays two straight lines, each representing one chemical species. This correlation map shows the properly sheared data and the projected spectrum. Figure 6(C) shows the standard image (phase encoding in the transverse direction), which is blurred due to the superposition of two spheres. Figure 6(D) shows the selective images

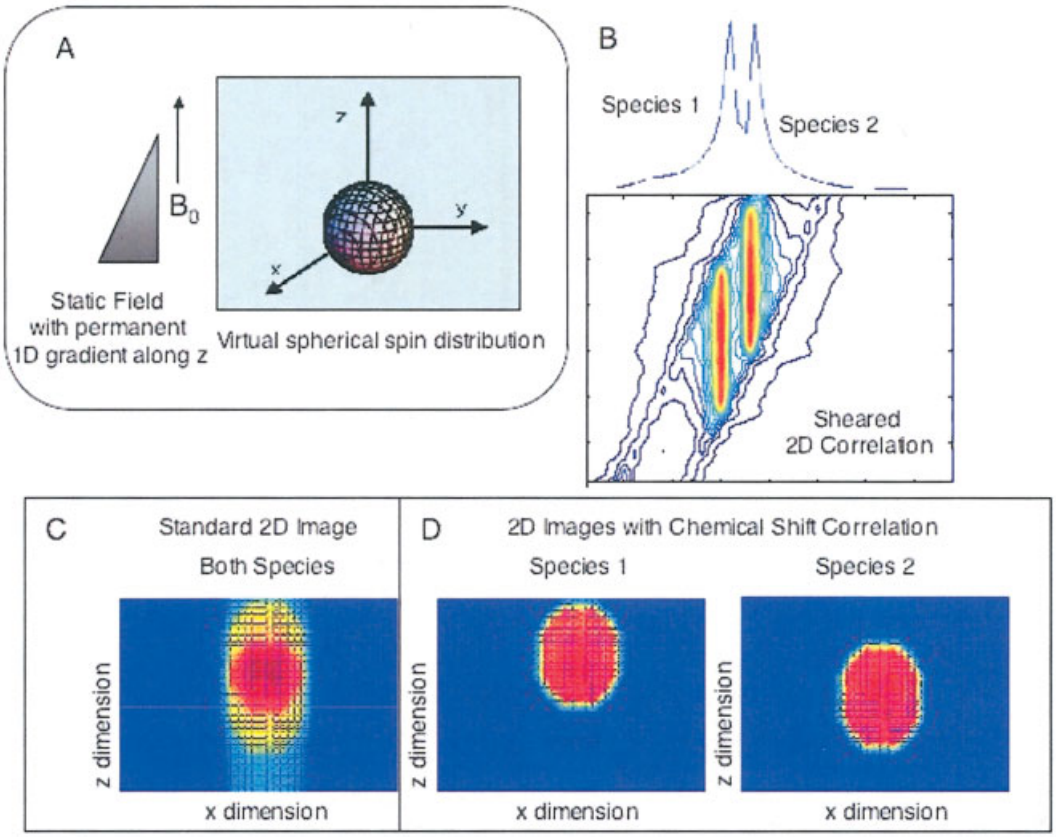

Figure 6 Simulated correlation results of a spherical virtual spin distribution of two chemical species. (A) Top left: the sample is assumed to be in the presence of a static field (4.2 T) with a constant gradient along the z direction (G_z = 2 G/cm). The excitation field is assumed to also have a constant gradient along the same direction. All the parameters for the simulations were set according to the experimental values. (B) Top right: the 2D subset (scaling and direct dimension) after shearing shows two lines, corresponding to the two different chemical species. The projection of the data gives a two-peak spectrum. (C) Bottom left: the standard image (phase encoding in the transverse direction) is blurred as a result of the superposition of two "spheres." (D) Selective images of the individual species. The images are the same, only shifted in frequency in the direct dimension. [Color figure can be viewed in the online issue, which is available at www.interscience.wiley.com.]

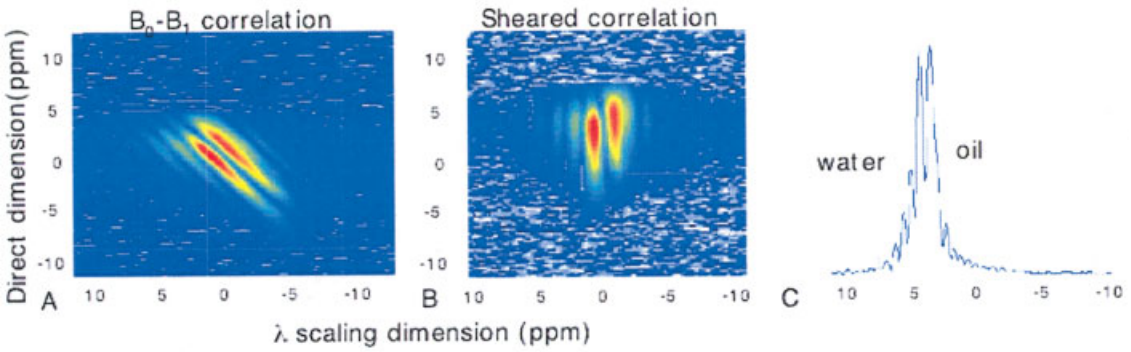

Figure 7 (A) The direct and scaling dimensions are selected to yield the correlation of the B_1 field and the static magnetic field. They show linear correlation indicated by the two lines for both chemical species. (B) The sheared data showing that the spectrum can be recovered upon projection. (C) The recovered spectrum of the water and oil sample (chemical shifts not referenced, but the spacing is 4 ppm, as expected). Oscillations are truncation artifacts of the Fourier transform. [Color figure can be viewed in the online issue, which is available at www.interscience.wiley.com.]

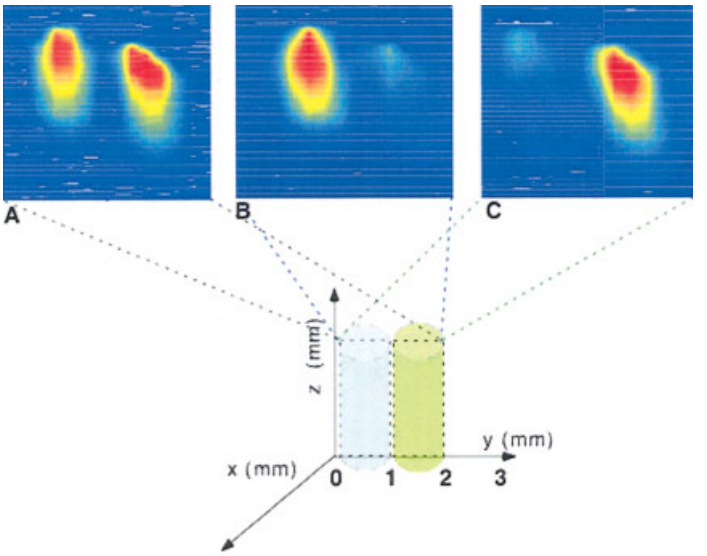

Figure 8 YZ projections and two-dimensional images of the sample (as a subset of the 3D data set) correlated with chemical shift. (A) Both tubes are shown at the 3 ppm trace. (B) The water image is shown at the 5 ppm trace. (C) The oil image is shown at the 1 ppm chemical shift trace (again, these shifts are not referenced). [Color figure can be viewed in the online issue, which is available at www.interscience.wiley.com.]

of the individual species. The images are the same, only shifted in frequency in the direct dimension.

RESULTS

Using the setup in Fig. 4 and the pulse sequence described earlier (Fig. 5), we recovered the full chemical shift dimension, as well as a two-dimensional image, of two capillary tubes (1 mm diameter and 3 mm length), one filled with water and the other with mineral oil. Figure 7(A) depicts the correlation of B_0 with B_1 by using the direct and the λ scaling two-dimensional subset of the three-dimensional data. The correlation is linear, as expected because of the matching of the RF and static fields, and two lines are distinct, one for each chemical species present in the sample. A first-order phase correction or shearing transformation is then applied to this 2D data set before the final Fourier transform with respect to t_1 to remove the tilting in (ω_1, ω_2) and produce $S'(t'_1,\omega')$ (Fig. 7[B]) (*20*). The sheared data upon projection produce the high-resolution proton chemical shift spectrum of water and oil (Fig. 7[C]).

$$S'(t'_1,\omega') = e^{i\phi(t_1,\omega_2)} = S(t_1,\omega_2), \text{ and } \phi(t_1,\omega_2) = \text{slope } \omega_2 t_1 \quad [2]$$

Figure 8 shows the spectrum-correlated two-dimensional images. Both cylinders are shown, along with water and oil images upon their chemical shift selection. Two 2D data sets are selected for the values of the scaling dimension for the different chemical shifts observed.

CONCLUSIONS

This article describes the design and construction of a model ex-situ system for spectroscopic imaging. We present chemical shift-selected sagital images (i.e., with one of the imaging dimensions being away from the sample via application of an ex-situ imaging sequence in a system where the sample is external to both the RF and imaging gradient coils). The extension to a truly single-sided system is expected to be straightforward with the present experimental configuration of RF and gradients coils. The double-opposed gradient coils were carefully designed to produce only transverse gradients even though they are single sided and have a natural field decrease with distance from their surface. This was accomplished by having two identical coils placed at a set distance and being run with opposite currents. This idea can be extended in designs different than the one selected here. We are currently working in the next step, which is single-sided systems and larger sample dimensions, where the nonlinearities of the gradients need to be

considered. For this experiment, based on a combination of the matching and shimming approach, work is underway (*9*, *13*).

REFERENCES

1. Eidmann G, Savelsberg R, Blumler P, Blümich B. 1996. The NMR MOUSE: A mobile universal surface explorer. J Magn Reson A 122:104–109.
2. Guthausen G, Guthausen A, Balibanu F, Eymael R, Hailu K, et al. 2000. Soft-matter analysis by the NMR MOUSE. Macromol Mater Eng 276/277:25–37.
3. Prado P, Blümich B, Schmitz U. 2000. One-dimensional imaging with a palm size probe. J Magn Reson 144:200–206.
4. Blümich B, Blumler P, Eidmann G, Guthausen A, Haken R, Schmitz U, et al. 1998. The NMR MOUSE: Construction, excitation, and applications. Magn Reson Imaging 16:479–484.
5. Casanova F, Blümich B. 2003. Two-dimensional imaging with a single-sided NMR probe. J Magn Reson 163:38–45.
6. Murphy DP. 1995. Advances in MWD and formation evaluation for 1995. World Oil 216(4):39–49.
7. Freedman R, Morris CE. 1995. Processing data from an NMR logging tool. Paper presented at the 70th SPE Annual Technical Conference and Exhibition. Dallas, Texas, October 22–25.
8. Kenyon WE, Howard JJ, Sezinger A, Straley C, Matteson A, Horkowitz K, et al. 1989. Pore size distribution and NMR in microporous cherty sandstones. Transactions of the SPWLA 30th Annual Logging Symposium. Denver, Colorado, June 11–14.
9. Meriles CA, Sakellariou D, Heise H, Moule AJ, Pines A. 2001. Approach to high-resolution ex situ NMR. Science 293:82–85.
10. Meriles CA, Sakellariou D, Pines A. 2003. Broadband phase modulation by adiabatic pulses. J Magn Reson 164:177–181.
11. Demas V, Sakellariou D, Meriles C, Han S, Reimer J, Pines A. 2004. 3D phase encoded chemical shift MRI in the presence of inhomogeneous fields. Proc Natl Acad Sci USA 101(24):8845–8847.
12. Perlo J, Demas V, Casanova F, Meriles C, Reimer J, Pines A, et al. 2005. High-resolution NMR spectroscopy with a probable single-sided sensor. Science 308:1279.
13. Marble AE, Mastikhin IV, Colpitts BG, Balcom BJ. 2005. An analytical methodology for magnetic field control in unilateral NMR. J Magn Reson 174:78–87.
14. Perlo J, Casanova F, Blümich B. 2006. Single-sided sensor for high-resolution NMR spectroscopy. J Magn Reson 180:274–279
15. Topgaard D, Martin RW, Sakellariou D, Meriles CA, Pines A. 2004. "Shim pulses" for NMR spectroscopy and imaging. Proc Natl Acad Sci USA 101:17576.
16. Prado P. 2003. Single-sided imaging sensor. Magn Reson Imaging 21:397–400.
17. Perlo J, Casanova F, Blümich B. 2004. 3D imaging with a single-sided sensor: an open tomograph. Magn Reson 166:228–235.
18. Baril N, Thiaudiere E, Quesson B, Delande C, Canioni P, Franconi J. 2000. Single coil surface imaging using a radiofrequency field gradient. J Magn Reson 146: 223–227.
19. Fukushima E, Jackson JA. 2004. Unilateral magnet having a remote uniform field region for nuclear magnetic resonance. US patent 6,828,892.
20. Grandinetti PJ, Baltisberger JH, Llor A, Lee YK, Werner U, Eastman MA, et al. 1993. Pure-absorption-mode lineshapes and sensitivity in tow-dimensional dynamic angle spinning NMR. J Magn Reson A 103: 72–81.